



WiBend: Wi-Fi for Sensing Passive Deformable Surfaces

Mira Sarkis, Céline Coutrix, Laurence Nigay, Andrzej Duda

► To cite this version:

Mira Sarkis, Céline Coutrix, Laurence Nigay, Andrzej Duda. WiBend: Wi-Fi for Sensing Passive Deformable Surfaces. ICMI '19 2019 International Conference on Multimodal Interaction, Oct 2019, Suzhou, China. 10.1145/3340555.3353746 . hal-02413564

HAL Id: hal-02413564

<https://hal.science/hal-02413564>

Submitted on 16 Dec 2019

HAL is a multi-disciplinary open access archive for the deposit and dissemination of scientific research documents, whether they are published or not. The documents may come from teaching and research institutions in France or abroad, or from public or private research centers.

L'archive ouverte pluridisciplinaire **HAL**, est destinée au dépôt et à la diffusion de documents scientifiques de niveau recherche, publiés ou non, émanant des établissements d'enseignement et de recherche français ou étrangers, des laboratoires publics ou privés.

WiBend: Wi-Fi for Sensing Passive Deformable Surfaces

Mira Sarkis

Céline Coutrix

Gne.MiraSarkis@gmail.com

Celine.Coutrix@imag.fr

Univ. Grenoble Alpes, CNRS, Grenoble INP, LIG
38000 Grenoble, France

Laurence Nigay

Andrzej Duda

Laurence.Nigay@imag.fr

Andrzej.Duda@imag.fr

Univ. Grenoble Alpes, CNRS, Grenoble INP, LIG
38000 Grenoble, France

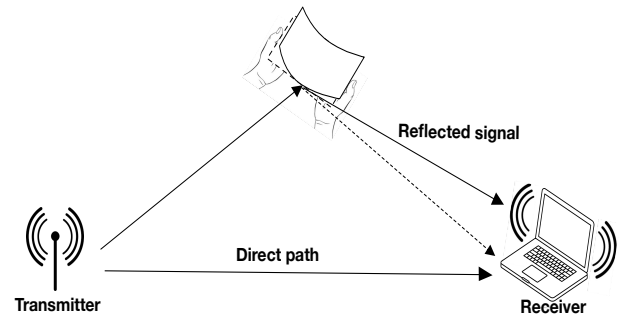
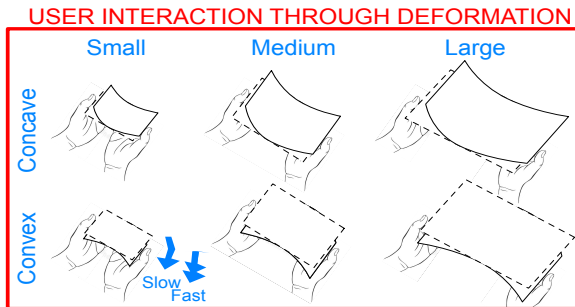


Figure 1: (Left) Interaction dimensions explored by WiBend: users can deform interactive surfaces of different size, at different speed, and with different bending direction. (Right) Principle of WiBend: bending a non-instrumented surface between a Wi-Fi transmitter and a Wi-Fi receiver. The device reflects the Wi-Fi signal and bending alters the reflection.

ABSTRACT

We present WiBend, a system that recognizes bending gestures as the input modalities for interacting on non-instrumented and deformable surfaces using WiFi signals. WiBend takes advantage of off-the-shelf 802.11 (Wi-Fi) devices and Channel State Information (CSI) measurements of packet transmissions when the user is placed and interacting between a Wi-Fi transmitter and a receiver. We have performed extensive user experiments in an instrumented laboratory to obtain data for training the HMM models and for evaluating the precision of WiBend. During the experiments, participants performed 12 distinct bending gestures with three surface sizes, two bending speeds and two different directions. The

performance evaluation results show that WiBend can distinguish between 12 bending gestures with a precision of 84% on average.

CCS CONCEPTS

- **Human-centered computing** → **Interaction devices**;
- **Computing methodologies** → *Machine learning*.

KEYWORDS

Deformable interfaces, sensing techniques, non-instrumented surfaces, bending, Wi-Fi signals, HMM.

ACM Reference Format:

Mira Sarkis, Céline Coutrix, Laurence Nigay, and Andrzej Duda. 2019. WiBend: Wi-Fi for Sensing Passive Deformable Surfaces. In *2019 International Conference on Multimodal Interaction (ICMI '19)*, October 14–18, 2019, Suzhou, China. ACM, New York, NY, USA, 10 pages. <https://doi.org/10.1145/3340555.3353746>

1 INTRODUCTION

Deformable surfaces define a vast set of emerging interaction modalities actively studied in Human-Computer Interaction (HCI). In particular, changes in size and curvature (Figure 1, left) amount to a large body of previous work. Previous work on deformable surfaces showed that changes in size [11, 20] and curvature [4, 13, 24, 26, 27] offer a great potential for interaction. Changes in size support scenarios in which users

Permission to make digital or hard copies of all or part of this work for personal or classroom use is granted without fee provided that copies are not made or distributed for profit or commercial advantage and that copies bear this notice and the full citation on the first page. Copyrights for components of this work owned by others than ACM must be honored. Abstracting with credit is permitted. To copy otherwise, or republish, to post on servers or to redistribute to lists, requires prior specific permission and/or a fee. Request permissions from permissions@acm.org.

ICMI '19, October 14–18, 2019, Suzhou, China

© 2019 Association for Computing Machinery.

ACM ISBN 978-1-4503-6860-5/19/05...\$15.00

<https://doi.org/10.1145/3340555.3353746>

switch between, e.g., a phone, a tablet, or a table-sized surface to accommodate their context of use, preferences, or applications. Changing curvature supports scenarios in which users bend their interactive surface, to, e.g., flip through pages, move the carret for text manipulation or trigger a weapon in a shooting game.

Existing techniques to implement deformable surfaces suffer from major drawbacks [16]. One approach requires cumbersome instrumentation of the surface itself, through, e.g., optical [12] or bend sensors [10, 16]. This approach results in fragile, thick, and hard-to-build prototypes.

Another approach, which we partially adopt in this study, is to instrument the environment proximal to the user [19, 25, 26]. On the one hand, this approach results in non-digital surfaces, also called non-instrumented or passive surfaces, and enables more robust and lightweight devices. On the other hand, this approach requires additional instrumentation of the environment with RGB and/or depth cameras [19, 25]. These techniques heavily depend on lighting conditions and occlusions. They also limit the space in which the user can interact and raise privacy concerns.

Contrastingly in this paper, we explore a non-intrusive use of Wi-Fi signals that already surround us, to recognize bending gestures with different size of surfaces. The resulting system, WiBend, allows for sensing passive deformable surfaces. WiBend does not require additional instrumentation of the environment as it takes advantage of existing deployments of Wi-Fi devices. Without any additional internal/external sensors, WiBend detects convex/concave bending gestures on three different sizes of deformable surfaces.

The challenge lies in the implementation of this gesture-based interaction modality by detecting bending gestures based on very noisy signals. Radio signals are strongly influenced by the environment in which they propagate, e.g., the objects they encounter, their shapes, their materials, and the speed at which a person or an object moves. While large scale activities (e.g., a person running, walking, or falling) were successfully detected in previous work [31], a bending gesture with a handheld passive surface is more challenging to recognize, as it is a small-scale activity. For instance, bending is usually short in time and requires limited amplitude and power.

In addition, for different users performing the exact same bending gestures, radio signals vary with respect to the amount of water, present in user bodies, that influences signal attenuation.

To overcome this difficulty, WiBend measures the Channel State Information (CSI) [36] of the 802.11n packet transmissions at 5.22 GHz. It then denoises CSI samples with a Principal Component Analysis (PCA) and extracts their features at different frequency resolutions and at different time scales with Discrete Wavelet Transform (DWT). WiBend uses the

features to represent different bending gestures in the form of Hidden Markov Models (HMM) [31] during a training phase, which results in a set of HMM models. During interaction, to recognize a gesture, WiBend extracts its features from CSI samples and computes their likelihood with respect to the pre-computed HMM models.

To train the HMM models, we designed an experiment with 37 participants performing interaction with a deformable surface. We explore the opportunities of detection through Wi-Fi signals for three parameters of the interaction:

- Surface size: small (20×13.5 cm or small tablet), vs. medium (32×22 cm or large tablet), vs. large (65×50 cm or a small table),
- Bending direction: convex vs. concave, and
- Bending velocity: slow vs. fast.

We found that WiBend classifies offline samples from 12 different gestures with a precision of 0.84 and a recall of 0.81 (i.e., only 0.19 of miss-rate) on average, in 200 ms.

The structure of the paper is as follows: we first explain the building blocks of WiBend to model and to recognize the bending gestures (Section 2). We then describe the experiment conducted in a laboratory (Section 3). Finally, we use the samples collected during the experiment to evaluate WiBend (Section 4). Finally, we position WiBend with respect to other existing recognition techniques (Section 5) and conclude (Section 6).

2 WIBEND: RECOGNIZING BENDING WITH WI-FI

Bending a deformable surface, in the presence of Wi-Fi signals generated by a transmitter, makes a part of the signal follow a longer path (see Figure 1, right). The deformable surface and the user body, including hands and forearms, behave as a reflector [15]: a part of the signal is dissipated and the rest is redirected in the space. The redirected signals contain all the information about the propagation space, e.g., user body, deformable surface, and hand movements.

The receiver of these signals can gather the information with great precision in the form of the Channel State Information (CSI) [36]. CSI refers to the measurements of the received signal properties (i.e., amplitude and phase) that characterize the wireless channel between a transmitter and a receiver. Figure 2 presents an example of CSI measurements corresponding to six repetitions of a bending gesture using a small surface. We can observe a repetitive pattern similar to an “M” that characterizes a bending gesture. This is one example of the effect of human gesture on Wi-Fi signals, that illustrates the interest of exploring Wi-Fi signals for recognizing bending gestures.

We build on previous work by Wang et al. [31] for detecting body movements to recognize bending interaction with Wi-Fi signals. While they used Hidden Markov Model (HMM)

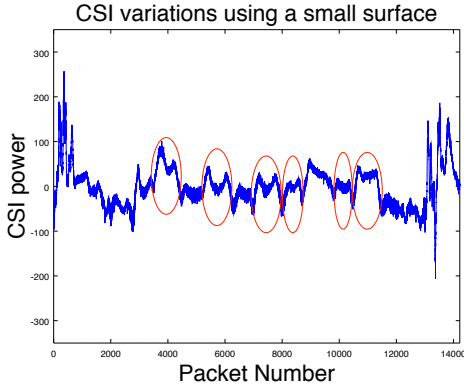


Figure 2: CSI variations for 6 repetitive concave bending gestures of a small surface (20×13.5 cm). Each circle corresponds to two gestures: bending and unbending.

to model full-body movements such as running, walking, or falling, we focus on the hand and forearm movements required to bend a deformable surface, which brings a new challenge: the reflection areas of arms and hands are small compared to the full body, thus the changes in CSI measurements are small and challenging to recognize.

Characterizing human activities, and more specifically bending gestures, requires the identification of: i) *duration* that corresponds to the time a user takes to perform a bending gesture; Duration is a design parameter of the interaction modality, and ii) *frequencies* that depend on the speeds at which radio signals propagates in the space following different paths, due to the body movements during the activity (i.e., the effect of moving each part of the body on the speed of the signal reflection).

By varying the bending speed as reported by Warren et al. [33], we can distinguish between slow and fast bending gestures since the gesture takes a longer time in the first case as compared to the second one. When switching between different surface sizes as in Xpaaand [11], users apply different forces represented by different frequencies to bend the larger surface as compared to the smaller one. Moreover, by combining different surface sizes and bending speeds, we can create several interaction profiles by jointly considering different frequencies and durations. Thus, it becomes possible to distinguish between a larger number of bending gestures.

Based on these considerations, WiBend operates in two phases as illustrated in Figure 3. It first extracts features related to the duration and the frequency of each interaction. In the second phase, WiBend constructs activity models. The building blocks of WiBend take advantage of two signal processing techniques (PCA, Principal Component Analysis and DWT, Discrete Wavelet Transform) and a machine learning algorithm (HMM).

Since our objective is to capture the dynamicity of CSI measurements, it is important to process data over time. Finding a relevant time window is important as it guarantees sufficient granularity to capture the changes in the environment without increasing the complexity of the machine learning algorithm. As the gesture durations are 600 ms and 1200 ms in our experiment, we have empirically found that a window of 200 ms provides enough granularity for activity recognition.

The input to WiBend are the CSI samples collected by the receiver and the output is a set of interaction models and a model for “No-Interaction”—this is the period during which a user was present but did not perform any bending gesture. We use these models: 1) to detect the presence of bending interaction and 2) to recognize the interaction characteristics (i.e., surface size, as well as bending speed and direction).

Signal Denoising with Principal Component Analysis

CSI measurements contain a lot of noise inherent to wireless transmissions. We can observe in Figure 2 high amplitude impulse and burst noise of CSI samples that overlay relevant signals corresponding to the information about bending interaction. As the receiver uses two antennas and the 802.11n transmission spreads information on 30 frequencies (i.e., OFDM sub-carriers [34]), we obtain 60 CSI values for each packet. However, the CSI values are correlated [31]: they are namely subject to the same noise and contain redundant information.

To denoise the measurements and remove redundancy, we apply a Principal Component Analysis (PCA). The first component contains the most correlated information [31], i.e., the noise. Thus, we eliminate it and retain the following 5 components that contain 85% of the signal information.

Feature Extraction with Discrete Wavelet Transform

After PCA, we extract frequency components at different time scales to obtain interaction features. With the Discrete Wavelet Transform (DWT), we can achieve a good trade-off in time and frequency (i.e., high time resolution for fast interaction and high frequency resolution for slow interaction). In addition, DWT reduces the data size, which makes them more suitable for the machine learning algorithm used for model construction and for interaction recognition.

For each window of 200 ms, we apply DWT with 11 levels to decompose the five principal components. We then average the resulting coefficients over the principal components. Each of our feature vectors contains 25 values representing three types of information:

- the energy at each wavelet level representing the intensity of movements with different speeds (11 features),

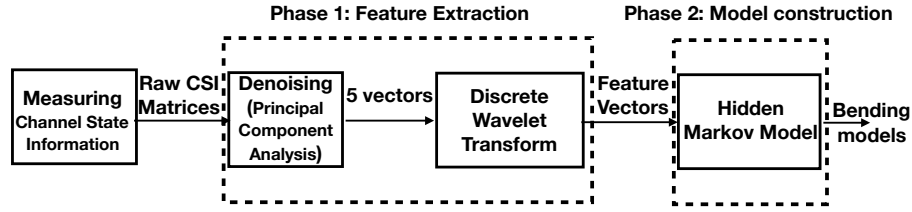


Figure 3: Building blocks for CSI processing and modelling bending gestures.

- the difference at each level between two consecutive windows representing the continuous temporal evolution of user interaction (11 features),
- three estimated speeds corresponding to hand and arm movements assuming that user legs and torso are static during each interaction (3 features).

To estimate the speeds, we use the percentile method with 0.25, 0.5, and 0.75 of the total energy as thresholds. They respectively correspond to a slow hand movement, a fast movement, and a fast movement with the biggest surface. For the last case, we consider that more force and energy are required to bend the largest surface, thus it can be better distinguished.

Learning and Recognizing Interaction: Hidden Markov Model

The features extracted from DWT draw a temporal pattern specific to each interaction. Thus, we can represent bending gestures as Markov models with hidden states.

As stated in the introduction section, we consider 3 parameters for designing the bending interaction, i.e., 3 surface sizes, 2 bending directions and 2 velocities. The 3 parameters result in 12 different bending gestures to be modelled using HMMs. Before building the models, we have to fix the number of states for each model. We had heuristically iterated between 2 and 20 states and selected the number of states that provides the best cross-validation accuracy [2]. Indeed, we focus in this paper on the WiBend accuracy rather than on its performance. A higher number of states results in more complex HMM models requiring a longer processing time. Finally, we initialized the state variables (i.e., mean vector, covariance matrix and transition probabilities of HMM) based on the training dataset obtained during the experiment described in the next section.

3 EXPERIMENT

The objectives of the experiment are two-fold: 1) gather data to construct the 12 HMM models corresponding to 12 bending gestures and 2) evaluate the accuracy of WiBend in recognizing different bending gestures.

We run the experiment in a laboratory instrumented with an optical tracking system [21]. The point here is to ensure uniformity amongst participants while doing the gestures, especially when it comes to the gesture speed that is a classification parameter. Each experiment consisted of 12 steps in which each user performed different monitored interaction gestures with a deformable surface, fully crossing the following variables:

- (1) *bending direction*: convex and concave bending (see Figure 1).
- (2) *bending speed*: slow ($Mean = 1200$ ms) and fast ($Mean = 600$ ms) with a standard deviation $SD = 200$ ms. We compute the speed from the average time corresponding to the 6 bending gestures executed per user and per experiment step.
- (3) *surface size*: small (20×13.5 cm), medium (32×22 cm), and large (65×50 cm).

During the experiment, we consider that: 1) participants are mainly moving their arms and front-arms while bending a surface, 2) there is no interference from other participants, 3) participants are always positioned in the middle between two PCs. The constraints were required for the design of WiBend and the calibration of its parameters and models.

We have recruited 37 participants between 21 and 39 years old ($Mean = 26$ years old, 10 women and 27 men). They did not receive any compensation for participating in the study.

For the flexible surfaces, different materials can be used like cork, PVC, textile, papers amongst others. They do not attenuate the Wi-Fi signals but reflect them. Conductive materials, like aluminium, require further exploration as they attenuate the reflected signal. Because of experimental constraints, we dropped PVC as it reflects the IR light, misleading the Optitrack detection. Textile sheets are loose and difficult to manipulate for bending.

We made three rectangular surfaces 2 mm thick out of flexible cork boards in the three sizes. The experiments took place in a $6.08 \text{ m} \times 5.9 \text{ m} \times 2.5 \text{ m}$ room equipped with an Optitrack optical 3D tracking system [21] based on infrared cameras. We have placed three reflective markers at three positions on the surface: two on the two edges of the top front

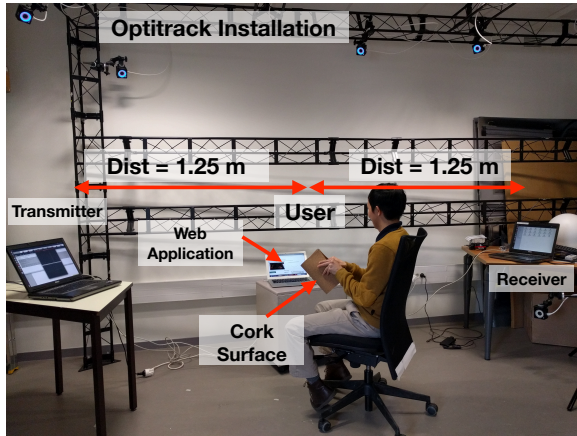


Figure 4: The participant holds the non-instrumented surface made of cork. He sits 1.25 m away from the transmitter and the receiver within the capture space of Optitrack. The participant synchronizes with the SVG animation presented by the Web application.

side of the surface and one in the middle. The experiment room also contained other electronic devices and objects: a 3D printer, two connected smart phones, an interactive tabletop, chairs, and tables. This defines a challenging environment especially because electronic devices are potential sources of interference that can alter CSI data, thus justifying the pre-processing of collected data.

To measure CSI values, we have used two PCs configured to work respectively as a transmitter and as a receiver. They run Ubuntu 14.04.4 kernel and used the Intel 5300 network interface card with two antennas. The two devices are placed at a distance of 3 m (see Figure 4). With a growing distance between the user and the PCs, the radio signal is attenuated and noise increasingly interferes with the signal. Thus, we need an efficient denoising method such as PCA—it eliminates the component that usually contains the maximum redundant information, i.e., noise in our case. We set the distance between devices based on a trial phase during which we varied the distance by up to 4 meters in a room. The resulting signals showed clear M patterns proving the potential of using Wi-Fi signals for bending gesture recognition.

We have deployed a CSI measuring tool [7] on the receiver wireless driver to collect and record signal measurements. We have configured the transmitter to send 802.11n packets at 5.22 GHz at a transmission rate of 1 kHz (1 packet every 1 ms) to capture even the shortest bending interaction.

We have developed a Web application with a Node.js server to guide the participants during the experiment (see Figure 5 for a screenshot of the Web application): 1) We collected demographics of participants (name, age, and gender). 2) We explained the experimental procedure and the

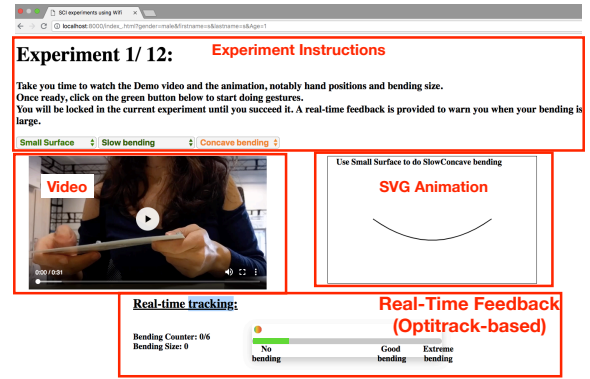


Figure 5: Screenshot of the Web application user interface during the experiment.

three variables for each experiment step. 3) For each step, the application displayed the values of the three variables and illustrated them using videos together with SVG animations. The animation speed corresponds to the required bending speed and aims at assisting participants during the experiment. 4) The application provided participants with real-time feedback about the bending size and speed, using Optitrack.

Participants sat in a chair at the center between the transmitter and the receiver (see Figure 4). We first introduced the participants to the experiment and instructed them to follow the bending speed. Participants practiced on fitting bending speed prior to each step. The order of presentation of the 2 bending speeds and of the 2 bending directions was random, while we proposed the three surfaces according to their increasing size. For each of the 12 configurations, we asked participants to repeat each gesture six times. We tracked the bending gestures with Optitrack. We notified the participants to stop bending and to start unbending till flat, when the range of the bending movement reached a threshold value that we heuristically set to 75% of the surface width. This extreme position corresponds to having both sides of the surface parallel to each other. If the participant correctly followed the bending speed (i.e., a range of speeds), the application logged the corresponding CSI measurements. Otherwise, we asked the participant to perform the gestures again. The interest here is to ensure that slow bending is never confused with fast bending, otherwise resulting CSI data will incorrectly be labeled, thus affecting WiBend performance for recognizing the different interaction speeds.

In total, the experiment took between 15 and 25 minutes per participant with a success rate varying on average between 75% and 95% per experiment. For each successful gesture, we collected the consecutive 3D positions of the markers on the surface during the bending movement, together with the consecutive CSI measurements.

Table 1: WiBend classification results using precision, recall and miss-rate, for HMM models with 16 states.

<i>Model</i>	<i>Recall</i>	<i>Precision</i>	<i>MissRate</i>
16 States			
Large FastConcave	0.95	0.82	0.05
Large FastConvex	0.79	1	0.21
Large SlowConcave	0.89	0.63	0.11
Large SlowConvex	0.50	1	0.50
Medium FastConcave	0.74	0.87	0.26
Medium FastConvex	0.89	0.8	0.11
Medium SlowConcave	0.68	0.71	0.31
Medium SlowConvex	0.68	0.64	0.32
Small FastConcave	0.89	0.81	0.11
Small FastConvex	0.94	0.78	0.06
Small SlowConcave	0.61	1	0.39
Small SlowConvex	1	0.90	0
“No-Interaction”	1	0.86	0
Average	0.81	0.84	0.19

We collected $37 \times 12 = 444$ bending samples, in addition to 51 samples corresponding to CSI measurements in the presence of a user standing still (i.e., absence of bending gestures) and in the presence of the electronic devices including a running 3D printer. These samples labeled “No-Interaction” were collected during 5 days at different hours. The aim here was to evaluate the performance of WiBend in detecting the presence or not of bending gestures.

Finally, we divided the obtained dataset of 495 samples (444 bending + 51 “No-Interaction” samples) into two parts: 248 samples for training, constructing and validating the HMM models and 247 samples for testing them. We estimated that 247 samples are representative of the variability between participants (i.e., body constituents and attitudes) and the variability in the way of executing gestures,

4 WIBEND EVALUATION

To evaluate WiBend, we compute the amount of true positives (TP), false positives (FP), and false negatives (FN). We then use *Precision* and *Recall* defines as follows:

$$Precision = \frac{TP}{TP + FP} \quad (1) \quad Recall = \frac{TP}{TP + FN} \quad (2)$$

Precision represents the proportion of the data samples that our model detects as corresponding to one model that actually do correspond to this model. Recall expresses the ability of our models to find all relevant instances in a dataset. MissRate complements recall and represents the proportion of the data samples WiBend could not identify correctly. We compute these values using the testing dataset dedicated to the evaluation.

Prior to this step, we first select the number of states (from 1-20) for the HMM models that will be used for testing

WiBend, using 10-fold cross-validation method, which resulted in selecting models with 16 states for testing WiBend.

Table 1 shows the detailed classification results for the 13 activities including “No-Interaction”. WiBend can classify the different activities with on average a precision of 0.84 and a recall of 0.81 (MissRate of 0.19). Table 1 also shows that WiBend can distinguish “No-Interaction” from bending gestures with a recall of 1 and a precision of 0.86. These values can ensure that no interaction (e.g., modifying the displayed items) will be performed in the absence of users or in the absence of bending gestures.

To obtain a deeper understanding of the achieved classification, we use a confusion matrix to identify the most frequently misplaced classes of gestures.

A confusion matrix is two-dimensional and has as many rows and columns as there are classes, i.e., 13 in our case. The columns represent the true classifications and the rows represent the system classifications. If the system performs perfectly, there will be scores only in the diagonal cells. If the system has any misclassifications, they are indicated in the off-diagonal cells. Figure 6 presents the heatmap of the normalized confusion matrix corresponding to our 13 activities (e.g., 12 gestures and no interaction). Note that the matrix diagonal represents the recall values also presented in Table 1.

LargeFastConcave, SmallSlowConvex, SmallSlowConvex have recall values higher than 0.94 and precision values higher than 0.78.

For gestures (i.e., LargeFastConvex, LargeSlowConvex, SmallSlowConcave) in Table 1 for which the precision value is 1 (i.e., 100% of hits), MissRate values are high (i.e., respectively 0.21, 0.50 and 0.39).

LargeFastConvex is mostly detected as LargeFastConcave and MediumFastConcave in 5% of the cases, and as LargeSlowConcave in 11% of the cases.

LargeSlowConvex is detected as LargeFastConcave and LargeSlowConcave each in 6% of the cases, as MediumFastConvex, MediumSlowConvex and SmallFastConvex each in 11% of the cases.

LargeSlowConvex gesture is the most difficult type of gestures for users to perform because it required a good control of the large surface and extra effort to maintain a slow speed while doing the convex bending.

SmallSlowConcave is detected as MediumSlowConcave in 22% of the cases, MediumSlowConvex in 6% and No-Interaction in 11% of the cases.

It is remarkable that gestures performed using the small surface are never confused with gestures performed using the large surface. The rectangle at the top left side of Figure 6 highlights this point: 4×4 zeros representing the absence of false positives.

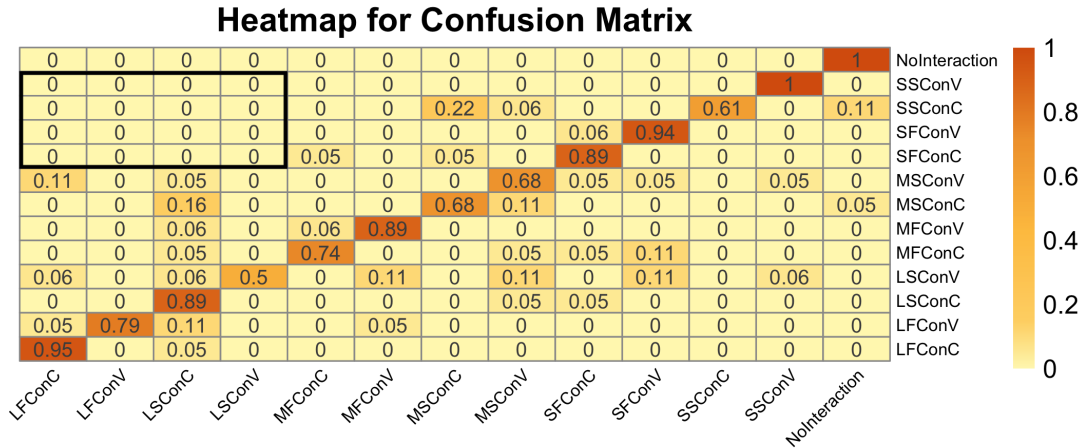


Figure 6: Heatmap representation of the Confusion Matrix. Classnames follow the XYConZ pattern in which X refers to surface size: Large, Medium, or Small, Y refers to speed: Fast or Slow, and ConZ refers to bending direction (ConCave or ConVex).

Gestures done using a medium size surface are being confused with gestures done equally using large and small surface sizes. For instance, MediumSlowConvex gestures are confused in total in 16% (i.e., $0.11+0+0.05+0$) of the cases with gestures done with a large surface versus 15% (i.e., $0.05+0.05+0+0.05$) with a small surface. Note that Small Slow-Concave is confused in 22% of the cases with Medium Slow-Concave. Thus, using a small or medium surface to do a SlowConcave gesture does not make a difference when using WiBend. Moreover, WiBend achieves good precision and recall values (i.e., higher than 75%) for simple HMM models with 10 states.

Finally, WiBend takes 200 ms on the average (after 10 iterations) to recognize a bending gesture. This value is promising for real-time recognition required for WiBend interaction (e.g., modifying the display on the surface or sending a command to connected objects in the environment according to the recognized gesture).

WiBend Limitations and Usage Scenarios

Currently, WiBend cannot distinguish between multiple users, which would require multiple access points to collect more data. We therefore envision usage scenarios with only one user interacting at a given time. In a surgery room, the use of non-sterilizable electronic devices is not possible. The staff can use a non-instrumented surface as it can be sterilized. For instance, using a surgical navigation system such as the OrthoPilot system [3], the staff member can bend the surface forwards and backwards to browse through the steps of the surgery workflow.

In a museum, each painting has a dedicated space and a non-instrumented surface is attached to each painting. A user in front of a painting bends the surface to visualize the lower layers of paint on top of it or on a dedicated display

next to it. In this public context, using a non-instrumented and cheap surface as a means of interaction has the benefit of being robust and tolerant to theft.

5 RELATED WORK

WiBend builds on previous work in the field of deformable interfaces and sensing techniques based on radio signals.

Deformable User Interfaces

Deformable user interfaces take advantage of the physical deformation of an object as a form of input or output [18, 24].

In particular, WiBend focuses on changes in size [5, 11, 20], bending direction [8], and speed [8, 33]. WiBend adopts existing interaction techniques to contribute with a novel technique for recognizing bending gestures involving non-instrumented surfaces. While changes in size were proven to be relevant for both input and output [5, 11, 20], both bending direction and speed were found to be relevant in a previous user elicitation study [33].

Other relevant dimensions are the location of the bend (e.g., top corner, side, bottom corner), the size of the bending area, and the angle of bending. We have left the aspects related to the location, the size of the bending area, and the angle of bending for future work, as these dimensions bring further challenges for sensing with Wi-Fi signals.

Sensing Approaches for Deformable Surfaces

We have found two main sensing approaches to dealing with deformable surfaces in the literature. In the first approach, the surface itself embeds sensors to track deformations [13, 23]. For instance, PaperPhone is a flexible surface with 5 bend sensors and a classifier based on K-nearest neighbors for detecting bending gestures [13].

The second approach dissociates the sensing technique from the interaction surface by deploying sensors in the environment to track deformations. WiBend belongs to this approach, which involves a lightweight interactive surface. Contrary to WiBend, most previous work proposed to use camera-based tracking systems. For instance, Gallant et al. [6] proposed a deformable surface with reflective markers tracked with an infrared camera.

Ex-hibit [20] and Xpaaand [11] both used reflective markers and an infrared camera-based system to track the changes in size of the deformable surface. Leal and Schaefer [14] used a Vicon motion tracking system (with 8 cameras) to reconstruct 3D points corresponding to a deformable surface. Flexpad [26] uses a Kinect depth sensor to track deformations on a simple, non-instrumented deformable surface, while disambiguating user hands from the surface deformation. Cobra [35] mixes both approaches as its plastic board is equipped with 4 bend sensors, 2 pressure sensors, and 4 infrared LEDs tracked by a distant Wii Remote.

Such approaches require the environment to be instrumented with dedicated tracking systems, which limits the use of a deformable surface to a dedicated space. In contrast, WiBend uses ambient radio signals and the widespread communication infrastructure to overcome the limitation and to eliminate the need for tagging deformable surfaces with trackable markers.

Backscatter and RFID for Deformable Surfaces

Recent work tends to reduce the size and complexity of objects such as sensors by eliminating the need for batteries. An example is the design of 3D printed wireless sensors [9] made of plastic only and able to modulate Wi-Fi signals to transmit the sensed information. Compared to RFID that requires a specific equipment to receive and decode signals, such an approach [9] uses commonly used smartphones to decode information. This kind of design makes the decoding of the object state straightforward, but it requires that objects follow design constraints, especially for embedded antennas, to properly backscatter radio signals. In contrast, WiBend does not focus on the design of objects but rather on detecting interaction with *non-instrumented* objects. To our knowledge, there is no existing work that enables external sensing of deformable surfaces using an existing widespread infrastructure without constraining the surface design.

Human Activity Detection with Wi-Fi

In contrast to techniques such as WiSee [22] and WiTrack [1] that require modified WiFi hardware and specialized software for user tracking, several initiatives, e.g., WiHear [28], CARM [31], proposed to use commercial WiFi access points.

Such recent studies focused on the analysis of CSI measurements for tracking human movements [30–32, 36] or recognizing lip movements as in WiHear [28].

Similar to WiBend, these systems consist of extracting features from CSI and applying machine learning techniques to build models and classifiers. Their authors used different machine learning and classification techniques such as logistic regression, support vector machines (SVM), Hidden Markov Models (HMM) [31], and deep learning [36].

Wang et al. used HMM to model user activities [31] (i.e., sequence of temporal states) such as running, walking, falling amongst others. While these activities consist of moving torso and legs, WiBend applies this approach to hand and forearm movements with promising results. WiBend uses heuristic methods to determine threshold values for distinguishing front-arm movements from torso and legs.

Wang et al. [29] also used Wi-Fi to recognize handwriting in the air and Ma et al. [17] to identify sign language gestures. While these previous studies focused on hand and forearm movements like WiBend, their setups required an array of antennas or/and multiple receivers. Contrastingly, WiBend uses a single transmitter and a single receiver, which corresponds to a common network deployment.

6 CONCLUSION

In this paper, we have described WiBend, a system to recognize bending gestures of passive deformable surfaces with Wi-Fi signals. This work is a first step towards accomplishing the Internet of Interactive Things (IIoT) that takes advantage of physical non-digital objects for interaction. Non-digital objects can define interaction modalities: their manipulation by users will be recognized through radio signals. We have performed an extensive user experiment in an instrumented laboratory to obtain data for training the HMM models and evaluate the precision of WiBend for 12 different bending gestures performed by 37 participants. The results show that WiBend achieves an average precision greater than 84%. In addition, it can distinguish between two different movement speeds, three surface sizes, and bending directions. First however, we plan to set up application scenarios in which we will be able to evaluate qualitatively the reactivity of WiBend from the user perspective.

ACKNOWLEDGMENTS

This work has been supported by the French Ministry of Research projects PERSYVAL-Lab (ANR-11-LABX-0025-01), AP2 (ANR-15-CE23-0001) and AN@TOMY2020 (ANR-16-CE38-011).

REFERENCES

- [1] Fadel Adib, Zachary Kabelac, Dina Katabi, and Robert C. Miller. 2014. 3D Tracking via Body Radio Reflections. In *Proceedings of the 11th USENIX Conference on Networked Systems Design and Implementation (NSDI'14)*. USENIX Association, Berkeley, CA, USA, 317–329. <http://dl.acm.org/citation.cfm?id=2616448.2616478>
- [2] Sylvain Arlot et al. 2010. A survey of Cross-Validation Procedures for Model Selection. *Statistics surveys* 4 (2010), 40–79.
- [3] Aesculap. Company Bbraun. 2019. OrthoPilot Navigation system. <https://www.bbraun.com>.
- [4] Victor Cheung, Alexander Keith Eady, and Audrey Girouard. 2018. Deformable Controllers: Fabrication and Design to Promote Novel Hand Gestural Interaction Mechanisms. In *Proceedings of the Twelfth International Conference on Tangible, Embedded, and Embodied Interaction*. ACM, 732–735.
- [5] Céline Coutrix and Cédric Masclet. 2015. Shape-change for zoomable tuis: Opportunities and limits of a resizable slider. In *Human-Computer Interaction*. Springer, 349–366.
- [6] David T Gallant, Andrew G Seniuk, and Roel Vertegaal. 2008. Towards More Paper-like Input: Flexible Input Devices for Foldable Interaction Styles. In *Proceedings of the 21st annual ACM symposium on User interface software and technology*. ACM, 283–286.
- [7] Daniel Halperin, Wenjun Hu, Anmol Sheth, and David Wetherall. 2011. Tool Release: Gathering 802.11n Traces with Channel State Information. *ACM SIGCOMM CCR* 41, 1 (Jan. 2011), 53.
- [8] Felix Heibeck, Basheer Tome, Clark Della Silva, and Hiroshi Ishii. 2015. uniMorph: Fabricating Thin Film Composites for Shape-Changing Interfaces. In *Proceedings of the 28th Annual ACM Symposium on User Interface Software & Technology (UIST '15)*. ACM, New York, NY, USA, 233–242. <https://doi.org/10.1145/2807442.2807472>
- [9] Vikram Iyer, Justin Chan, and Shyamnath Gollakota. 2017. 3D Printing Wireless Connected Objects. *ACM Trans. Graph.* 36, 6, Article 242 (Nov. 2017), 13 pages. <https://doi.org/10.1145/3130800.3130822>
- [10] Lee Jones, John McClelland, Phonesavanh Thongsouksanoumane, and Audrey Girouard. 2017. Ambient Notifications with Shape Changing Circuits in Peripheral Locations. In *Proceedings of the 2017 ACM International Conference on Interactive Surfaces and Spaces (ISS '17)*. ACM, New York, NY, USA, 405–408. <https://doi.org/10.1145/3132272.3132291>
- [11] Mohammadreza Khalilbeigi, Roman Lissermann, Max Mühlhäuser, and Jürgen Steimle. 2011. Xpaaand: Interaction Techniques for Rollable Displays. In *Proceedings of the SIGCHI Conference on Human Factors in Computing Systems*. ACM, 2729–2732.
- [12] Kevin SC Kuang, Wesley J Cantwell, and Patricia J Scully. 2002. An Evaluation of a Novel Plastic Optical Fibre Sensor for Axial Strain and Bend Measurements. *Measurement Science and Technology* 13, 10 (2002), 1523.
- [13] Byron Lahey, Audrey Girouard, Winslow Burleson, and Roel Vertegaal. 2011. PaperPhone: Understanding the Use of Bend Gestures in Mobile Devices with Flexible Electronic Paper Displays. In *Proceedings of the SIGCHI Conference on Human Factors in Computing Systems*. ACM, 1303–1312.
- [14] Anamary Leal, Doug Bowman, Laurel Schaefer, Francis Quek, and Clarissa K Stiles. 2011. 3D Sketching using Interactive Fabric for Tangible and Bimanual Input. In *Proceedings of Graphics Interface 2011*. Canadian Human-Computer Communications Society, 49–56.
- [15] Vincent Liu, Aaron Parks, Vamsi Talla, Shyamnath Gollakota, David Wetherall, and Joshua R. Smith. 2013. Ambient Backscatter: Wireless Communication out of Thin Air. In *Proceedings of the ACM SIGCOMM 2013 Conference on SIGCOMM (SIGCOMM '13)*. ACM, New York, NY, USA, 39–50. <https://doi.org/10.1145/2486001.2486015>
- [16] Jessica Lo and Audrey Girouard. 2014. Fabricating Bendy: Design and Development of Deformable Prototypes. *IEEE Pervasive Computing* 13, 3 (2014), 40–46.
- [17] Yongsan Ma, Gang Zhou, Shuangquan Wang, Hongyang Zhao, and Woosub Jung. 2018. SignFi: Sign Language Recognition Using Wi-Fi. *Proc. ACM Interact. Mob. Wearable Ubiquitous Technol.* 2, 1, Article 23 (March 2018), 21 pages. <https://doi.org/10.1145/3191755>
- [18] Mie Nørgaard, Tim Merritt, Majken Kirkegaard Rasmussen, and Marianne Graves Petersen. 2013. Exploring the Design Space of Shape-Changing Objects: Imagined Physics. In *Proceedings of the 6th International Conference on Designing Pleasurable Products and Interfaces*. ACM, 251–260.
- [19] Simon Olberding, Sergio Soto Ortega, Klaus Hildebrandt, and Jürgen Steimle. 2015. Foldio: Digital Fabrication of Interactive and Shape-Changing Objects with Foldable Printed Electronics. In *Proceedings of the 28th Annual ACM Symposium on User Interface Software & Technology*. ACM, 223–232.
- [20] Michael Ortega, Jérôme Maisonnasse, and Laurence Nigay. 2017. EXHibit: a Mechanical Structure for Prototyping EXpandable Handheld Interfaces. In *19th International Conference on Human-Computer Interaction with Mobile Devices and Services (MobileHCI 2017)*. 4:1–4:11.
- [21] Natural Point. 2011. Optitrack. *Natural Point, Inc.*, [Online]. Available: <http://optitrack.com>. [Accessed 12 06 2018] (2011).
- [22] Qifan Pu, Sidhant Gupta, Shyamnath Gollakota, and Shwetak Patel. 2013. Whole-home Gesture Recognition Using Wireless Signals. In *Proceedings of the 19th Annual International Conference on Mobile Computing & Networking (MobiCom '13)*. ACM, New York, NY, USA, 27–38. <https://doi.org/10.1145/2500423.2500436>
- [23] Christian Rendl, David Kim, Sean Fanello, Patrick Parzer, Christoph Rhemann, Jonathan Taylor, Martin Zirkel, Gregor Scheipl, Thomas Rothländer, Michael Haller, et al. 2014. FlexSense: A Transparent Self-Sensing Deformable surface. In *Proceedings of the 27th annual ACM symposium on User interface software and technology*. ACM, 129–138.
- [24] Anne Roudaut, Abhijit Karnik, Markus Löchtefeld, and Sriram Subramanian. 2013. Morphees: Toward High "Shape Resolution" in Self-actuated Flexible Mobile Devices. In *Proceedings of the SIGCHI Conference on Human Factors in Computing Systems (CHI '13)*. ACM, New York, NY, USA, 593–602. <https://doi.org/10.1145/2470654.2470738>
- [25] Martin Schmitz, Jürgen Steimle, Jochen Huber, Niloofar Dezfouli, and Max Mühlhäuser. 2017. Flexibles: Deformation-Aware 3D-Printed Tangibles for Capacitive Touchscreens. In *Proceedings of the 2017 CHI Conference on Human Factors in Computing Systems*. ACM, 1001–1014.
- [26] Jürgen Steimle, Andreas Jordt, and Pattie Maes. 2013. Flexpad: Highly Flexible Bending Interactions for Projected Handheld Displays. In *Proceedings of the SIGCHI Conference on Human Factors in Computing Systems (CHI '13)*. ACM, New York, NY, USA, 237–246. <https://doi.org/10.1145/2470654.2470688>
- [27] Paul Strohmeier, Jesse Burstyn, Juan Pablo Carrascal, Vincent Levesque, and Roel Vertegaal. 2016. ReFlex: A Flexible Smartphone with Active Haptic Feedback for Bend Input. In *Proceedings of the TEI'16: Tenth International Conference on Tangible, Embedded, and Embodied Interaction*. ACM, 185–192.
- [28] Guanhua Wang, Yongpan Zou, Zimu Zhou, Kaishun Wu, and Lionel M. Ni. 2014. We Can Hear You with Wi-Fi!. In *Proceedings of the 20th Annual International Conference on Mobile Computing and Networking (MobiCom '14)*. ACM, New York, NY, USA, 593–604. <https://doi.org/10.1145/2639108.2639112>
- [29] Jue Wang, Deepak Vasisht, and Dina Katabi. 2014. RF-IDraw: Virtual Touch Screen in the Air Using RF Signals. In *ACM SIGCOMM Computer Communication Review*, Vol. 44. ACM, 235–246.

- [30] Wei Wang, Alex X. Liu, and Muhammad Shahzad. 2016. Gait Recognition Using Wifi Signals. In *Proceedings of the 2016 ACM International Joint Conference on Pervasive and Ubiquitous Computing (UbiComp '16)*. ACM, New York, NY, USA, 363–373. <https://doi.org/10.1145/2971648.2971670>
- [31] W. Wang, A. X. Liu, M. Shahzad, K. Ling, and S. Lu. 2017. Device-Free Human Activity Recognition Using Commercial WiFi Devices. *IEEE Journal on Selected Areas in Communications* 35, 5 (May 2017), 1118–1131. <https://doi.org/10.1109/JSAC.2017.2679658>
- [32] Y. Wang, K. Wu, and L. M. Ni. 2017. WiFall: Device-Free Fall Detection by Wireless Networks. *IEEE Transactions on Mobile Computing* 16, 2 (Feb. 2017), 581–594. <https://doi.org/10.1109/TMC.2016.2557792>
- [33] Kristen Warren, Jessica Lo, Vaibhav Vadgama, and Audrey Girouard. 2013. Bending the Rules: Bend Gesture Classification for Flexible Displays. In *Proceedings of the SIGCHI Conference on Human Factors in Computing Systems (CHI '13)*. ACM, New York, NY, USA, 607–610. <https://doi.org/10.1145/2470654.2470740>
- [34] Yiyang Wu and William Y Zou. 1995. Orthogonal Frequency Division Multiplexing: A Multi-Carrier Modulation Scheme. *IEEE Transactions on Consumer Electronics* 41, 3 (1995), 392–399.
- [35] Zi Ye and Hammad Khalid. 2010. Cobra: Flexible Displays for Mobile Gaming Scenarios. In *CHI'10 Extended Abstracts on Human Factors in Computing Systems*. ACM, 4363–4368.
- [36] Siamak Yousefi, Hirokazu Narui, Sankalp Dayal, Stefano Ermon, and Shahrokh Valaee. 2017. A Survey of Human Activity Recognition Using WiFi CSI. *arXiv preprint arXiv:1708.07129* (2017).